

Movie S1. Expected collective movements of cohesin hinge at the south interface, as deduced by normal mode analysis using ANM2.1. Atomic models of the wild-type mouse cohesin hinge appear yellow (SMC1) and green (SMC3). The model of the S568E mutant, which is equivalent to Psm3-A561E, one of the Cut1 suppressors, appears blue to red depending on the amplitude of movement (red indicating large movement). Both atomic models were generated by all-atom molecular dynamics simulations for 100 ns starting from the crystal structure of the wild type (PDB code: 2WD5). Purple broken lines show distances between residues on helix I of SMC1 (V622 and F630) and those on helix E (M573 and D565) of SMC3 in the mutant. This movie shows that the mutation causes much larger movements of helices A and E and those of coiled-coils connecting the hinge and the head domains of SMC3.

A *cut1/cut2* suppressors in cohesin

Suppressor genes	amino acid substitution	ts mutants used for screening
<i>psm3</i>	S127P	<i>cut1-A1816T</i>
<i>psm3</i>	G164D	<i>cut1-A1816T</i>
<i>psm3</i>	A561E	<i>cut1-L739S</i>
<i>psm3</i>	A561E	<i>cut1-A1816T</i>
<i>psm3</i>	P580H	<i>cut1-A1816T</i>
<i>psm1</i>	C626Y	<i>cut1-A1816T</i>
<i>psm1</i>	V646F	<i>cut1-L739S</i>
<i>psm1</i>	G661D	<i>cut2-R267Stop</i>
<i>rad21</i>	H42P	<i>cut2-R267Stop</i>
<i>rad21</i>	A53V	<i>cut1-A1816T</i>
<i>rad21</i>	T465P	<i>cut1-A1816T</i>
<i>rad21</i>	V594F	<i>cut1-A1816T</i>
<i>rad21</i>	V605F	<i>cut1-A1816T</i>
<i>mis4</i>	F616S	<i>cut1-A1816T</i>
<i>mis4</i>	P1035L	<i>cut1-A1816T</i>
<i>mis4</i>	L1188R	<i>cut1-A1816T</i>

B *rad21-K1* suppressors in cohesin

Gene	Amino acid substitution	Domain
<i>psm3</i>	K12E	ATPase
<i>psm3</i>	K118E	ATPase
<i>psm3</i>	S127Y/F	ATPase
<i>psm3</i>	K185I	CC
<i>psm3</i>	Y195S	CC
<i>psm3</i>	R199L/Q	CC
<i>psm3</i>	N971S	CC
<i>psm3</i>	F978L	CC
<i>psm3</i>	R985S	CC
<i>psm3</i>	F1021V/L	CC
<i>psm3</i>	G1099D	ATPase
<i>psm3</i>	A1133V	ATPase
<i>psm1</i>	R1127I	ATPase
<i>psm1</i>	Q1168E	ATPase

C *mis4-G1326E* suppressors in cohesin

Intergenic:		Intragenic:	
Gene	Amino acid substitution	Gene	Amino acid substitution
<i>psm3</i>	I20R	<i>mis4</i>	N348T
<i>psm3</i>	F41V/L	<i>mis4</i>	N584K
<i>psm3</i>	P69R	<i>mis4</i>	S642G
<i>psm3</i>	M74R	<i>mis4</i>	V648G
<i>psm3</i>	A76T	<i>mis4</i>	L654R
<i>psm3</i>	F82C	<i>mis4</i>	S782W
<i>psm3</i>	L98F	<i>mis4</i>	I803M
<i>psm3</i>	E108A	<i>mis4</i>	K807N/E
<i>psm3</i>	S1103A	<i>mis4</i>	T808I
<i>psm3</i>	C1116G	<i>mis4</i>	P810S/A/H
<i>psm3</i>	N1122T	<i>mis4</i>	E818K/A
<i>psm3</i>	C1127G/S	<i>mis4</i>	V819F
<i>psm3</i>	R1136C	<i>mis4</i>	Q822R/K
<i>psm3</i>	I1153L	<i>mis4</i>	D836A
<i>psm3</i>	C1154S	<i>mis4</i>	T837I
<i>psm3</i>	F1157L	<i>mis4</i>	D840Y/G
<i>psm3</i>	R1158W	<i>mis4</i>	T844R
<i>psm3</i>	E1187D/V	<i>mis4</i>	T869K
<i>psm1</i>	S162L	<i>mis4</i>	Q878K
<i>psm1</i>	A193V	<i>mis4</i>	H1044R
		<i>mis4</i>	Y1063C
		<i>mis4</i>	T1102P
		<i>mis4</i>	E1105Q
		<i>mis4</i>	S1212T
		<i>mis4</i>	L1231M
		<i>mis4</i>	L1246V
		<i>mis4</i>	H1306R
		<i>mis4</i>	F1316V/L
		<i>mis4</i>	C1332R
		<i>mis4</i>	M1343L
		<i>mis4</i>	S1346P
		<i>mis4</i>	N1354H/S
		<i>mis4</i>	T1359I
		<i>mis4</i>	A1383G
		<i>mis4</i>	S1385A
		<i>mis4</i>	D1387E
		<i>mis4</i>	I1415V

Table S1. Suppressors identified in cohesin. (A) Fifteen extragenic suppressors in the genes of cohesin subunits Psm1, Psm3 and Rad21, and in its loader Mis4, for *cut1* and *cut2* ts mutants were identified by whole-genome sequencing of spontaneous revertants isolated at the restrictive temperature. *psm3-A561E* was obtained twice as a suppressor of both *cut1-L739S* and *cut1-A1816T*. (B) Seventeen extragenic suppressors of *rad21-K1* ts mutant in *psm3* and *psm1*. Substituted amino acids were classified into 2 groups: mutations in the head domain of Psm3/Psm1 and mutations in the coiled coil (CC) of Psm3. (C) Suppressors of the *mis4-G1326E* ts mutant. Many were intragenic in *mis4* (right). Extragenic suppressors include 21 mutations in *psm3* head and 2 mutations in *psm1* head (left).

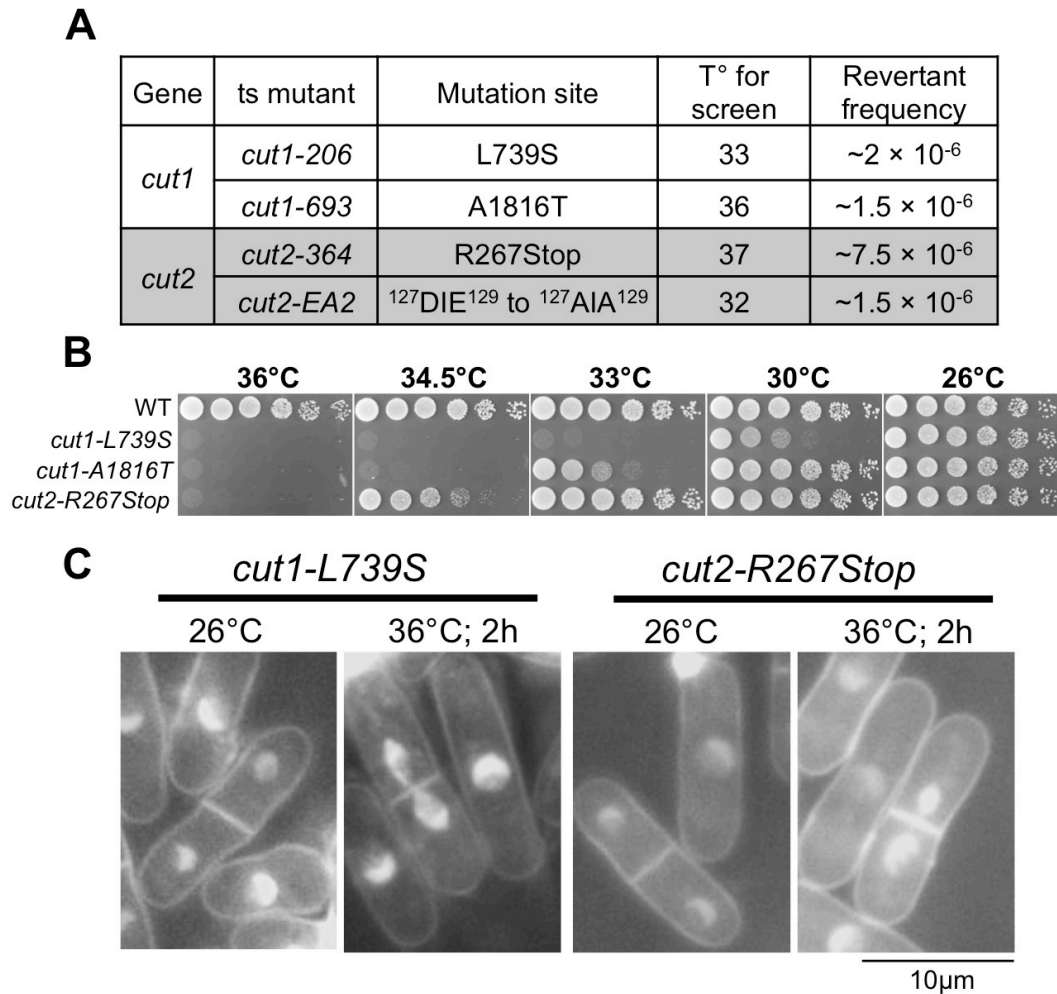


Fig. S1. Re-integration of *cut1* and *cut2* ts mutations into wild type. (A) Four *cut1* and *cut2* ts mutants used for suppressor screening. Their mutation sites were re-integrated into the *972h* wild type genome. Original strain numbers and the responsible mutations are indicated. Restrictive temperatures used for spontaneous revertants screening and their corresponding revertant frequencies are shown. **(B)** Spot test results for three re-integrated strains are shown at different temperatures. **(C)** DNA-specific fluorescent probe DAPI-stained *cut1-L739S* and *cut2-R267Stop* mutant cells are shown. They were cultured at the permissive temperature (26°C) and then shifted to the restrictive temperature (36°C) for 2 hr. Typical *cut1* and *cut2* phenotypes (undivided nuclei bisected by cytokinesis) were observed at 36°C.

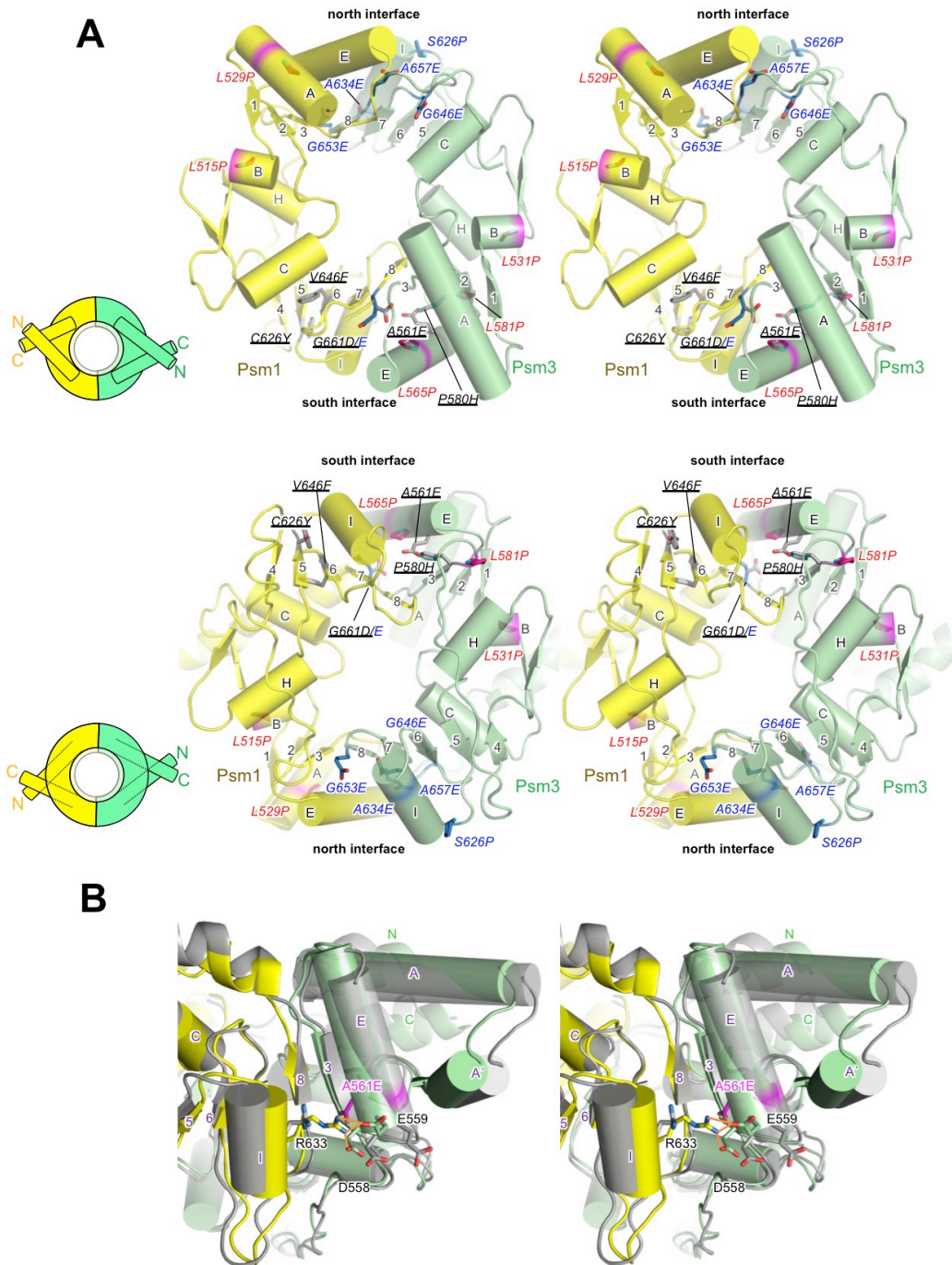


Fig. S2. Locations of *cut1* and *cut2* suppressors in the cohesin hinge and molecular simulation of the hinge for the Psm3-A561E mutation. (A) A stereo version of **Fig. 1B**. Top, top view of the hinge; bottom, bottom view. Yellow is used for Psm1 and green for Psm3. **(B)** A stereo version of **Fig. 1D**. Yellow and green are used for wild type and grey for the Psm3-A561E suppressor. Salt bridges between R633 in Psm1 and, D558 and E559 in Psm3 are shown with orange lines.

A	
Psm1 hinge (26 sites)	L485P, A495E, S496P, S502P, L515P, G524E, L529P, A540E, L545P, G546E, A551E, A560E, G598E, A599E, L601P, A619E, G621E, L624P, A632E, G657E, G661E, G662E, S663P, S664P, A669E, L680P
Psm3 hinge (33 sites)	L465P, L472P, L479P, L490P, S491P, L497P, G508E, G523E, G526E, L531P, A546E, G547E, L550P, L565P, G574E, L581P, L584P, A597E, L604P, A613E, S626P, A630E, A634E, L639P, L644P, G646E, G653E, A654E, L655P, A657E, G658E, S665P, L667P

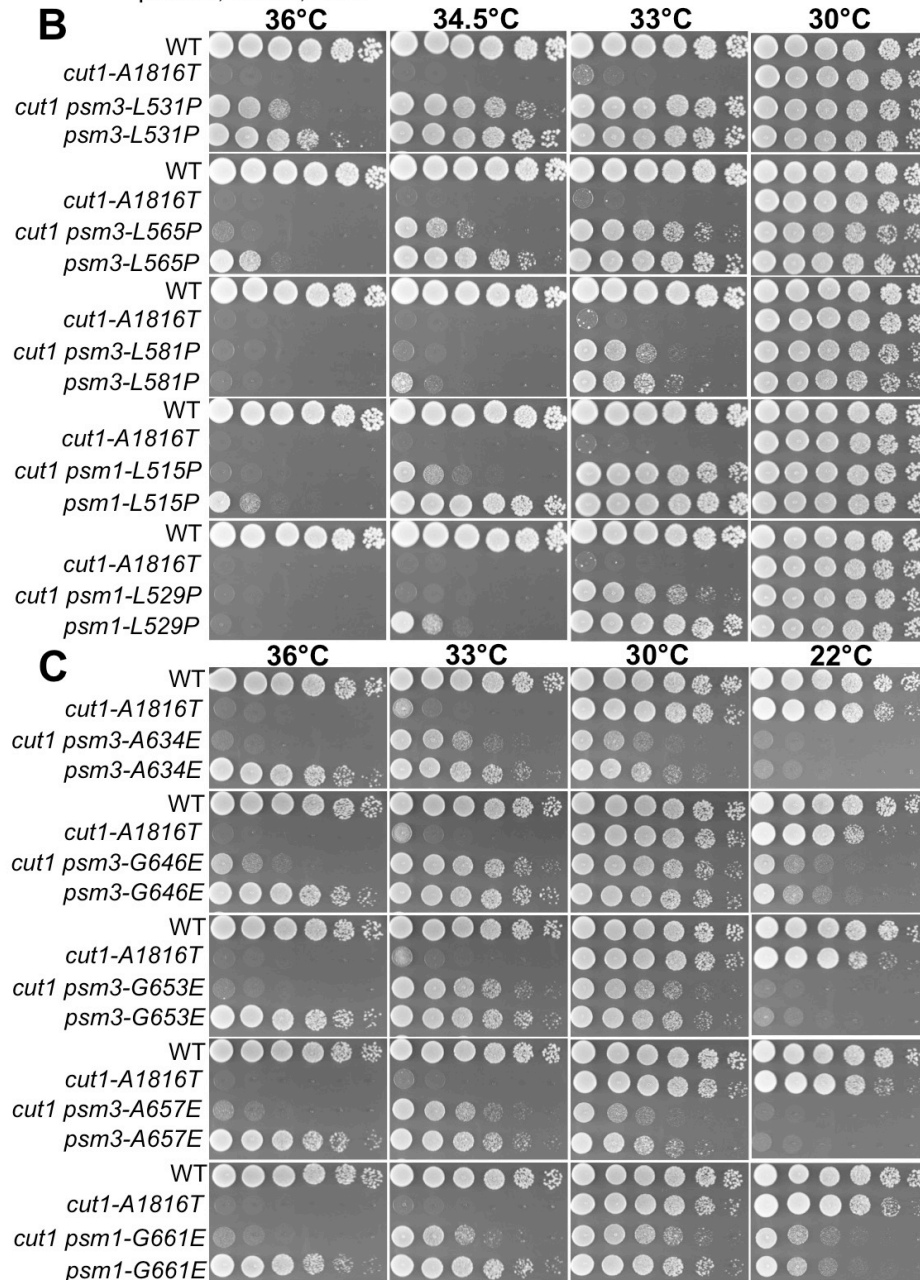


Fig. S3. Cohesin hinge ts/cs isolation and their suppression of *cut1*. (A) Single-site amino acid substitutions selected for site-directed mutagenesis targeted to cohesin hinge regions. (B) Suppression of *cut1* by cohesin hinge ts mutants identified from (A). (C) Suppression of *cut1* by cohesin hinge cs mutants identified from (A).

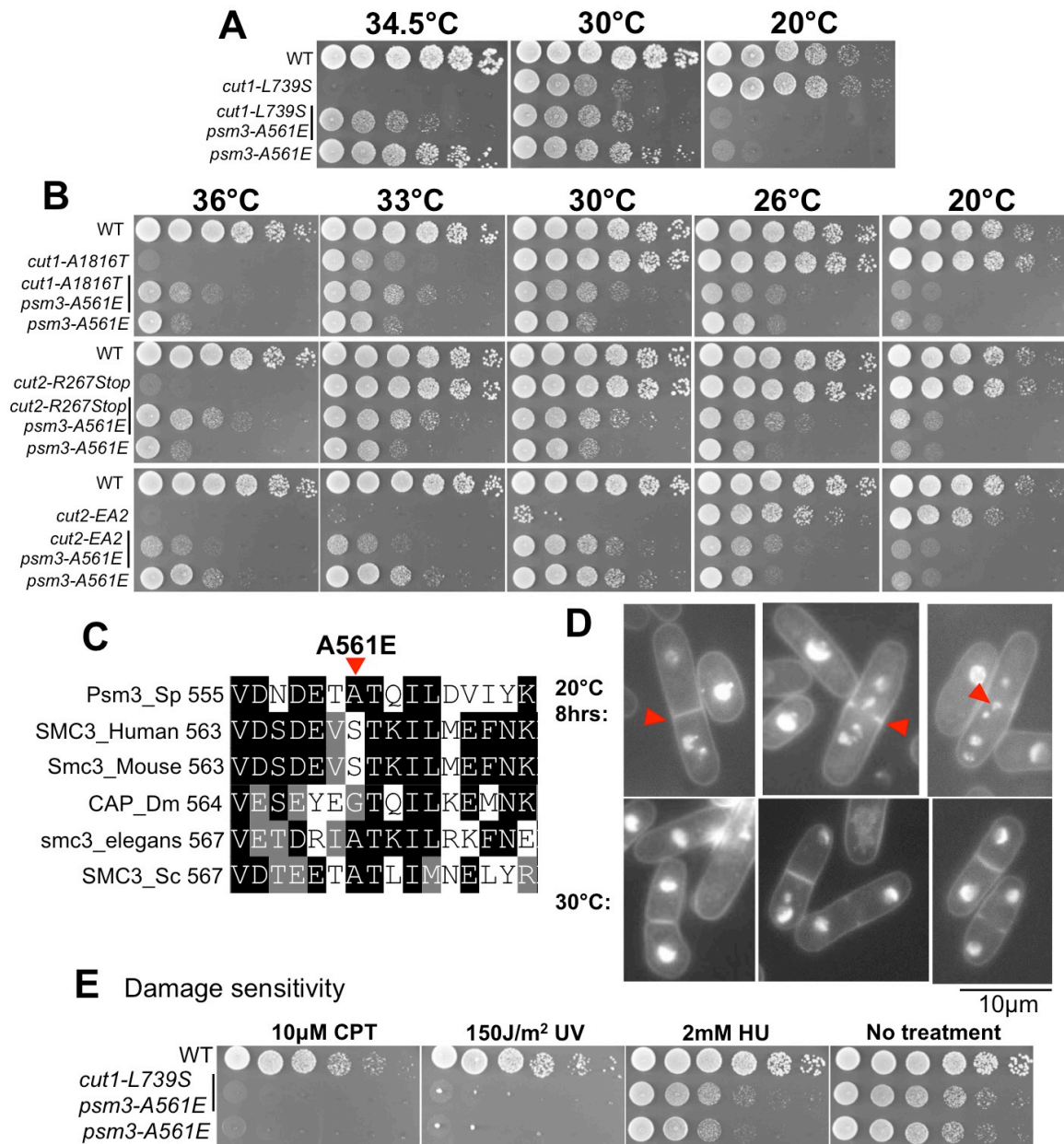


Fig. S4. Characterizations of *psm3-A561E*, a hinge-disrupting mutant. (A) Spot test result: *psm3-A561E* is cold sensitive (cs). No colony formation occurs at 20°C. The double mutant *cut1-L739S psm3-A561E* suppressed the ts phenotype of *cut1-L739S* at 34.5°C. (B) The cs mutant, *psm3-A561E*, rescued three other ts strains (*cut1-A1816T*, *cut2-R267Stop*, and *cut2-EA2*) too. (C) Amino acid sequence alignment of Psm3/SMC3 homologs among different organisms. (D) Cell culture phenotype of *psm3-A561E* at 30°C (permissive temperature) and after 8 hr at 20°C (restrictive temperature). Cells were stained with DAPI. Mitotic arrest occurred while sister chromatids were prematurely separated. (E) The *psm3-A561E* mutant produced a DNA damage-sensitive phenotype at the permissive temperature, regardless of the presence or absence of the *cut1-L739S* mutation. CPT, camptothecin; UV, ultraviolet irradiation; HU, hydroxyurea.

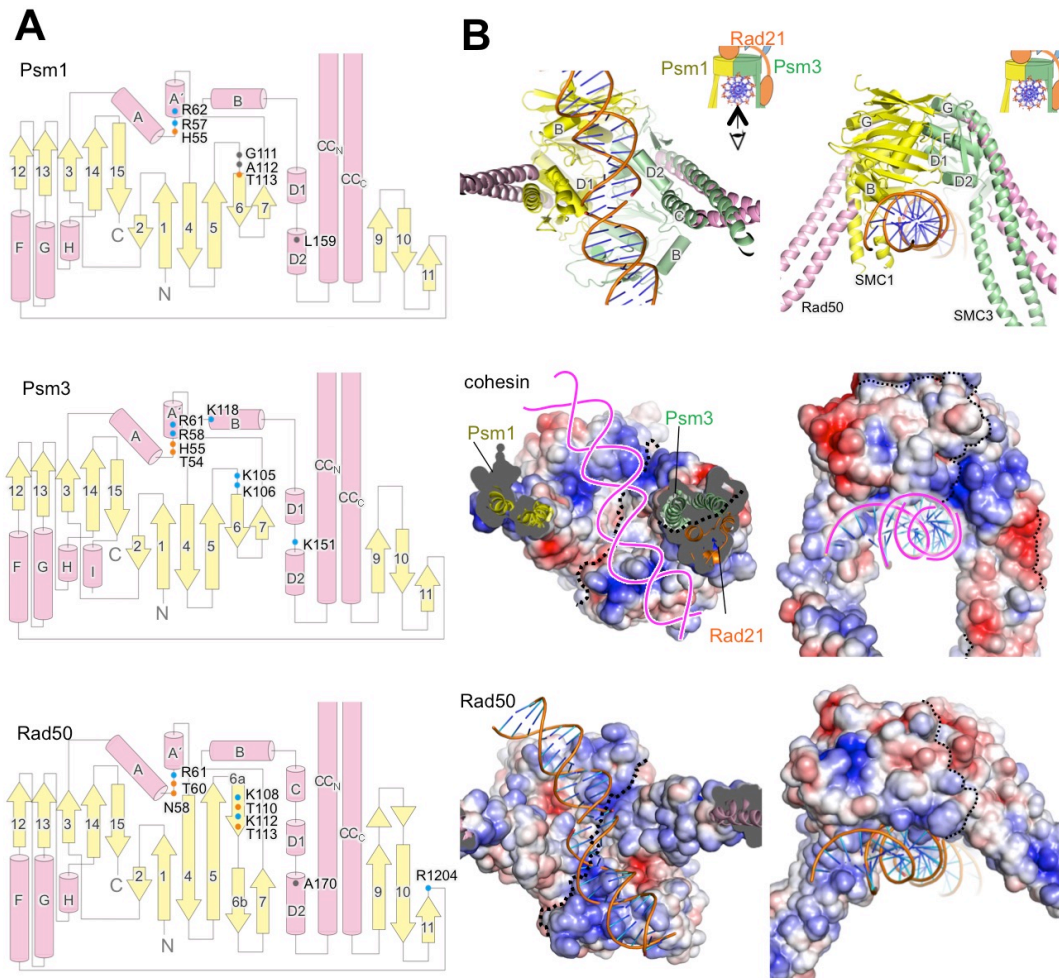


Fig. S5. Structural similarity of the heads between cohesin and Rad50, and putative DNA binding sites of cohesin. (A) Topology diagrams of the head for Rad50, Psm1, and Psm3. Residues that form salt bridges or hydrogen bonds with DNA in the crystal structure of DNA-bound Rad50 (PDB code 5DAC) are shown with circles. Residues, potentially contacting DNA, in Psm1/3 are also shown. (B) Electrostatic surface potential of the cohesin head with coiled coils, Rad21, and Rad50.

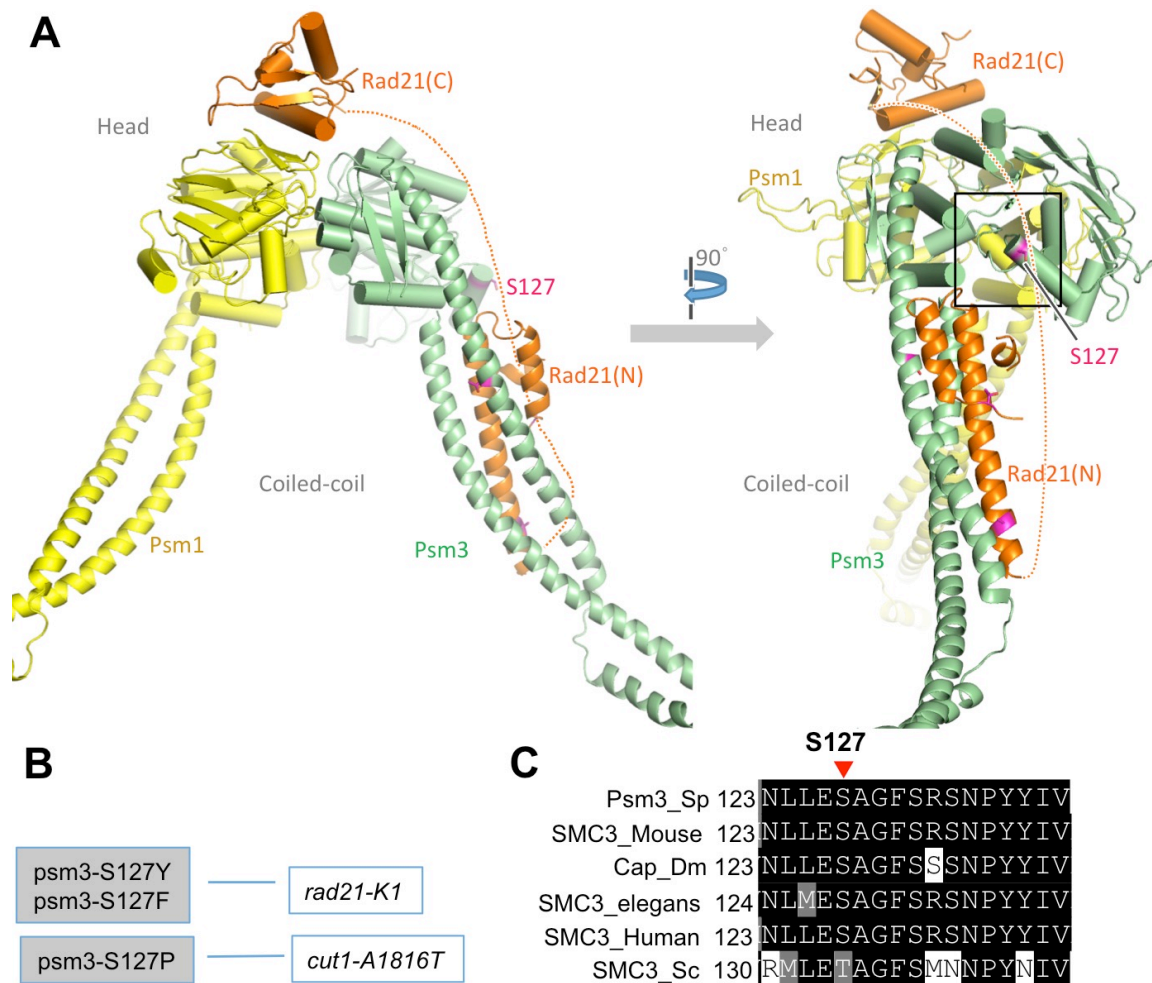


Fig. S6. Psm3 S127 is critical for the Psm3-Rad21 interaction. (A) Location of the residue, Psm3 S127, in the atomic structure of the Psm3 head domain (green). The right figure is rotated 90° in the clockwise direction. The dashed line indicates a hypothetical path that connects the N- and C-terminal regions of Rad21. **(B)** The *rad21-K1* mutant was suppressed by *psm3-S127Y/F*, while *cut1-A1816T* was suppressed by *psm3-S127P*. **(C)** Cohesin Psm3 S127 and its surrounding amino acids are conserved in budding yeast (Sc), *Caenorhabditis elegans*, *Drosophila melanogaster* (Dm), mouse, and human homologs.

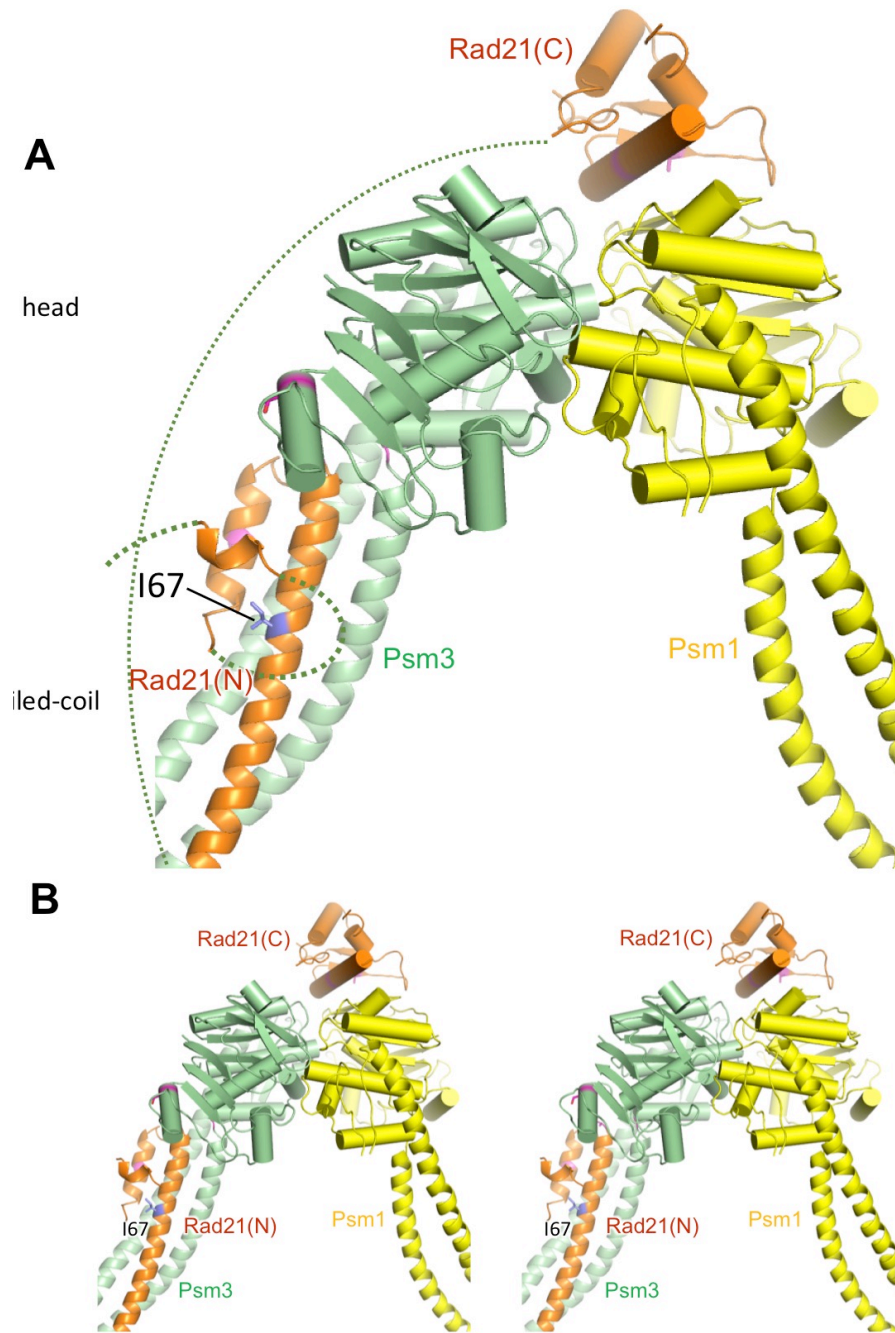


Fig. S7. Rad21 I67 in the cohesin structure. (A) Location of Rad21-I67 in the molecular structure. I67F is the effective mutation in *rad21-K1*. **(B)** Stereo view of the Rad21-I67 location.

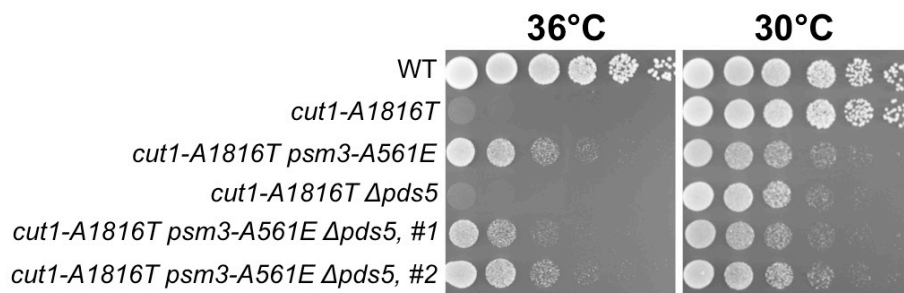


Fig. S8. Suppression of *cut1-A1816T* by *psm3-A561E* is Pds5 independent. Spot test results showing the genetic interaction among *cut1-A1816T*, *psm3-A561E* and $\Delta pds5$. Pds5 is not required for the suppression of the *cut1* mutant by *psm3-A561E*.

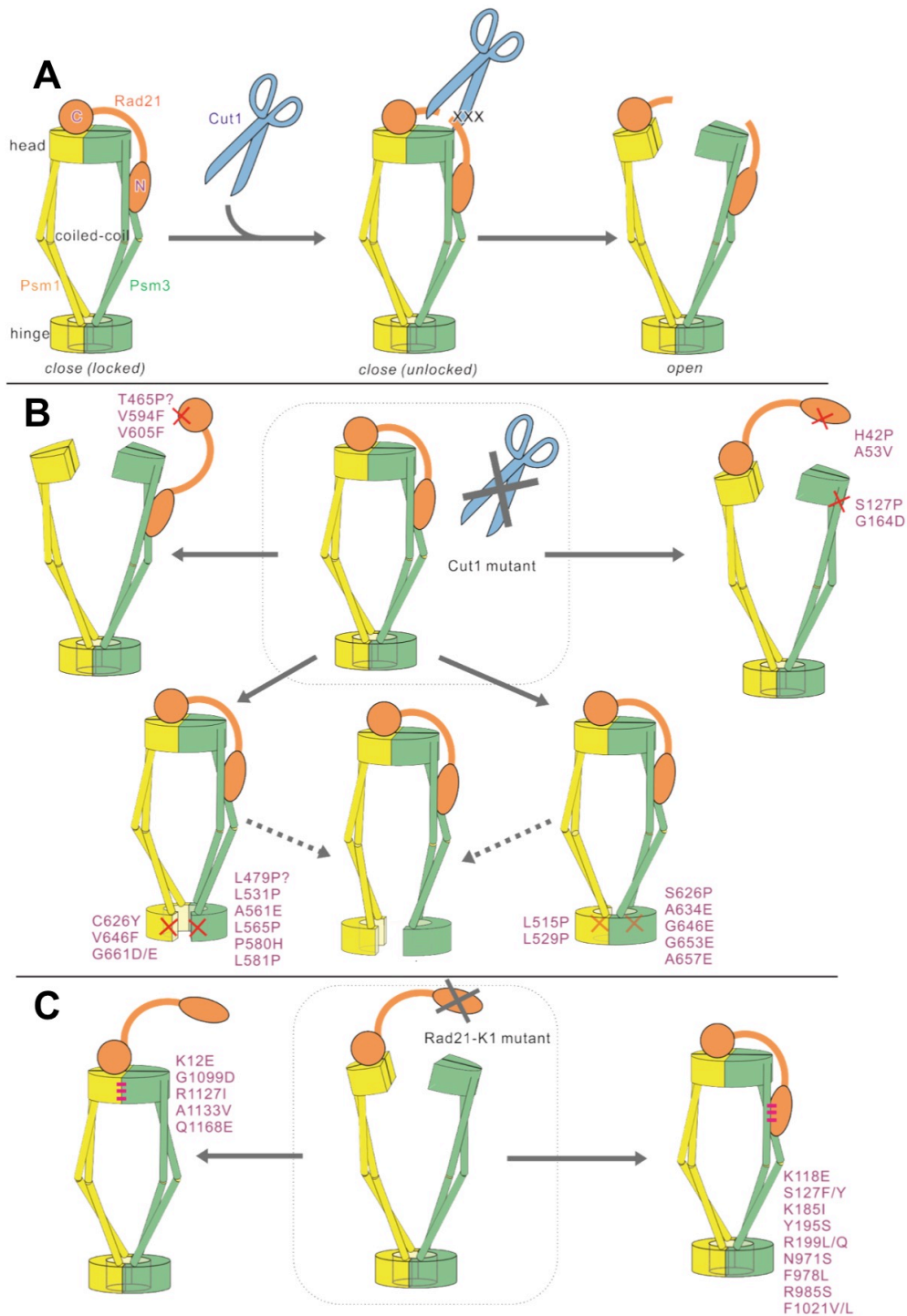


Fig. S9. Potential explanation of *cut1* and *rad21* suppressors through cohesin ring model. (A) Releasing of cohesin from DNA through Cut1 (Cut1 is represented as a pair of scissors) cleavage of Rad21 in normal (wild type) condition. **(B)** Releasing of cohesin from DNA through interface disruption in *cut1/cut2* revertants. **(C)** Restoration of cohesin-defective *rad21-K1* mutant by suppressors located in ATPase or coiled-coil domains of Psm3 and Psm1 (*SI Appendix, Table S1B*).

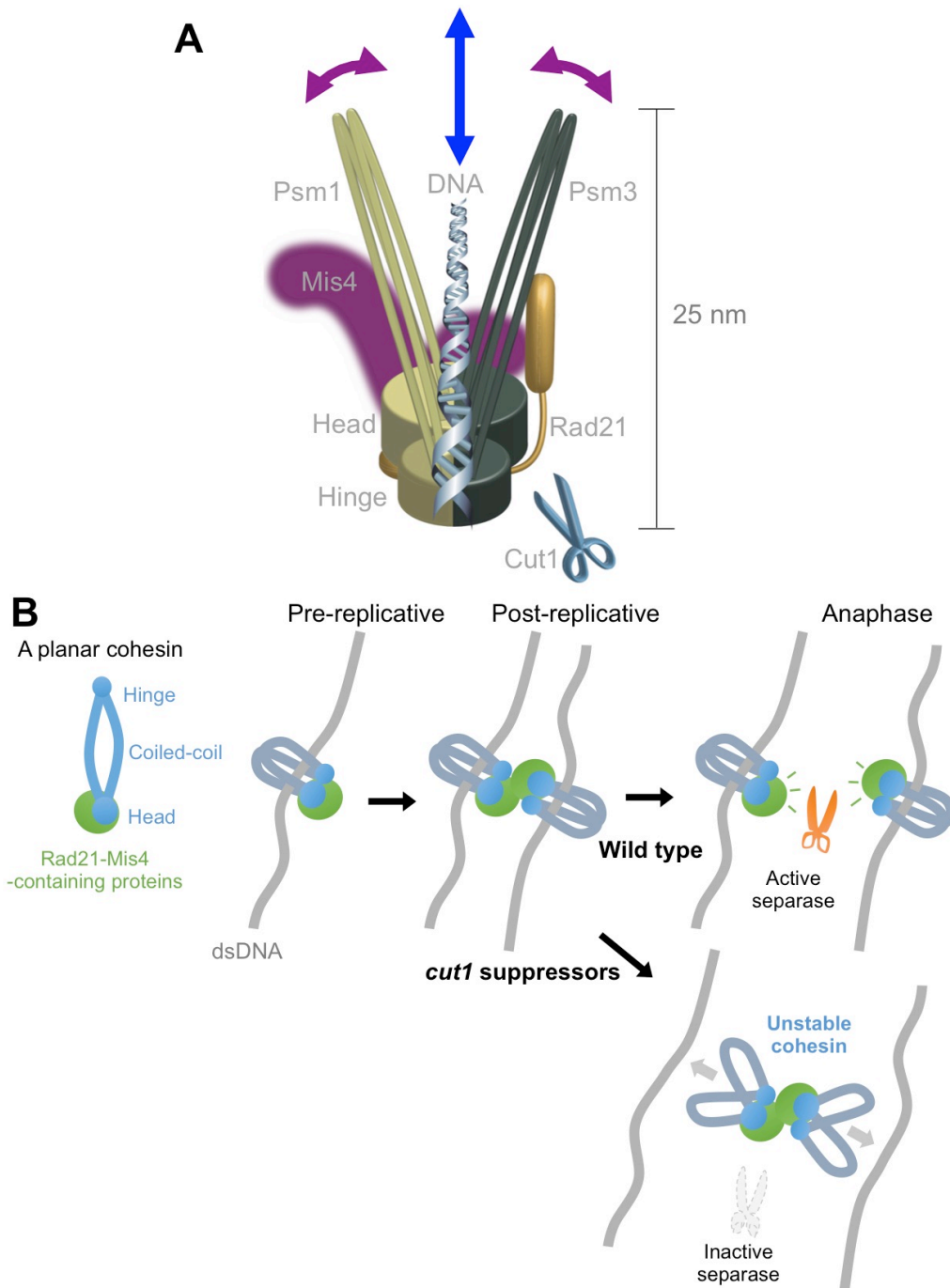


Fig. S10. A 'hold and release' model for cohesin-DNA interaction. (A) Arched coiled coil-mediated cohesin binding to or release from dsDNA. This 'hold and release' model is intended to explain cohesin's DNA interactions differently from the prevailing 'ring' model. The model fits to the tadpole like cohesin images reported (16, 48, 49). The cohesin head and coils may resemble Rad50, which binds to dsDNA via the DNA binding domain of head and the coiled-coils. The coiled-coil conformation under the control of the hinge and head is critical for binding to and releasing from DNA. Mis4 is a potential linker of two sister chromatids together with Rad21. **(B)** Model of 'hold and release' for sister chromatid cohesion. Since Rad21 cleavage is not required in *cut1* suppressors, opening of cohesin coiled-coil wings by *cut1* suppressors may release sister chromatids.